Impact of Wind on UAV Collision Avoidance

Sadvik Boddu*, Suraj Suman*, and Swades De†‡

*Department of Electrical Engineering, Indian Institute of Technology Patna, Bihar, 801106 India

† Department of Electrical Engineering, Indian Institute of Technology Delhi, New Delhi 110016, India

‡ Bharti School of Telecommunication, Indian Institute of Technology Delhi, New Delhi 110016, India

***Abstract*—Collision-free trajectory planning of UAVs is a challenging task. In this paper, we address the UAV collision avoidance problem in the presence of wind, which cannot be ignored in practical aerial-aided communication infrastructure deployment scenarios. In order to avoid a collision with an obstacle, the UAV needs to decide to make a turn from a sufficient distance at an appropriate angle, and this phenomenon is characterized by the two parameters termed as *turning radius* and *semiapex angle*. First, the effect of wind speed on the UAV movement is modeled, which is used to estimate the *turning radius* and *semiapex angle* in the presence of wind. The wind data is random in nature, so the collision avoidance parameters are also random. To this end, a discrete-time Markov chain model is used to analyze the collision avoidance parameters in a statistical sense. Finally, the probability of collision avoidance is estimated. For performance evaluation, the wind data of the last four years with five minutes resolution from three cities of the USA situated at diverse geographical locations is used. Through system simulations, the severity of collision performance in the presence of random wind is captured. Further, as a measure of collision avoidance, the turning radius and simplex angle are estimated as a function of wind velocity.**

***Index Terms*—Aerial-aided communication, collision avoidance, impact of wind, Markov chain, unmanned aerial vehicle (UAV)**

I. Introduction

Nowadays, unmanned aerial vehicles (UAVs), commonly known as drones, have become an appealing choice due to their unique features, such as scheduling of autonomous flight, excellent maneuverability, and payload-carrying capability. They are widely used in various applications, like military, cellular systems, logistics, healthcare, transportation, surveillance and monitoring, agriculture, remote automation, and disaster management [1]. The global commercial drone market is expected to grow at a compound annual growth rate of 13.9% from 2023 to 2030 [2]. However, the maximum hovering altitude of the UAVs is restricted. For example, in some countries, it is up to 120 m above the ground level [3], [4]. Due to this, the low altitude space allowed for UAV operation will have congested air traffic, which is a severe concern for safety, communication, and security [5]. In such a crowded airspace, ensuring the movement of UAV without any collision with other UAVs or surrounding infrastructure is a challenging task. Collision may have severe consequences, such as compromise with the safety of civilians, damage to the UAV and surrounding infrastructure, law and order issues, and degraded service quality to the end users. Therefore, designing a robust UAV collision avoidance mechanism by considering the practical deployment constraints is of major research interest. We address this issue in this work by considering the effect of wind.

A. Related Works

Cell and Non-cell-based methods are two approaches to establish a collision-free flight environment. A sequence of cells represents the flight environment in cell-based methods. A cell-based collision avoidance framework based on the Markov decision process is formulated in [6] to guide a team of UAVs. An optimal path search algorithm is developed in [7] for collision-free operation of UAVs. A varying cell strategy is presented in [8] by considering the aerodynamics constraints, where the avoidance actions are adapted to go through different cells. Various noncell-based techniques are also reported to establish a collision-free path. An analytically tractable potential field model of free space is reported in [9] to navigate the UAVs safely. A sense and avoid-based system is proposed in [10] to guarantee flight safety.

The work in [11] presents a method to avoid collision between UAVs using Wi-Fi beacons for transmitting position information to prevent collisions. This method comprises a UAV coordinate exchange protocol that encodes the positional information into the Wi-Fi service set identifier field. Geometry-based collision avoidance strategies for multiple UAVs are investigated in [12] using line-of-sight and relative velocity vectors. Here, each UAV determines the available plane and direction for collision avoidance. The work in [13] designed the safety radius in the presence of communication delays and estimation errors to avoid collision. A collision avoidance algorithm using a stereo vision sensor is presented in [14]. Here, the depth map information obtained from stereo vision detects an obstacle; subsequently, the collision-cone approach is adopted to avoid the collision. A statistically aided learning-based UAV localization is studied in [15] to aid collision avoidance and dense UAV swarm packing.

A two-stage reinforcement learning (RL) based multi-UAV collision avoidance approach is presented in [16], aiming to train a policy to plan a collision-free trajectory by leveraging local noisy observations. The policy using a supervised training method with a loss function is optimized in the first stage, whereas the policy is refined in the second stage. A deep reinforcement learning (DRL) based method is reported in [17] with obstacles in unstructured and unknown indoor environments. Here, the UAV can retain relevant information about the environment for better future navigation decisions. A probabilistic and DRL-based algorithm is presented in [18]

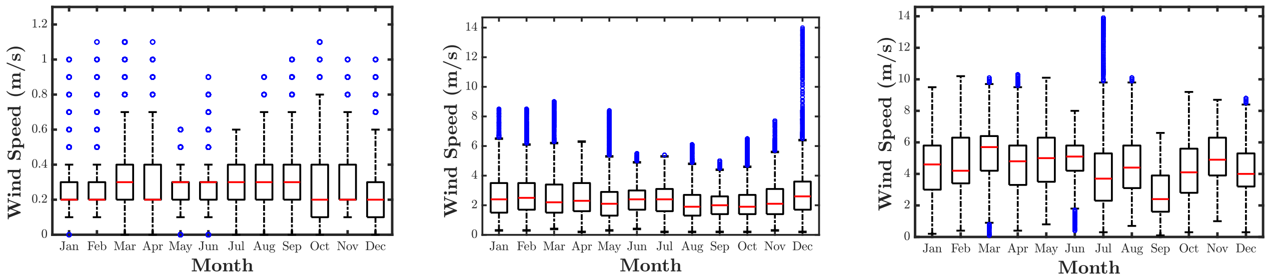

(a) Medford (Oregon) (b) Denver (Colorado) (c) Key West (Florida)

Figure 1: Variation of wind speed in different cities.

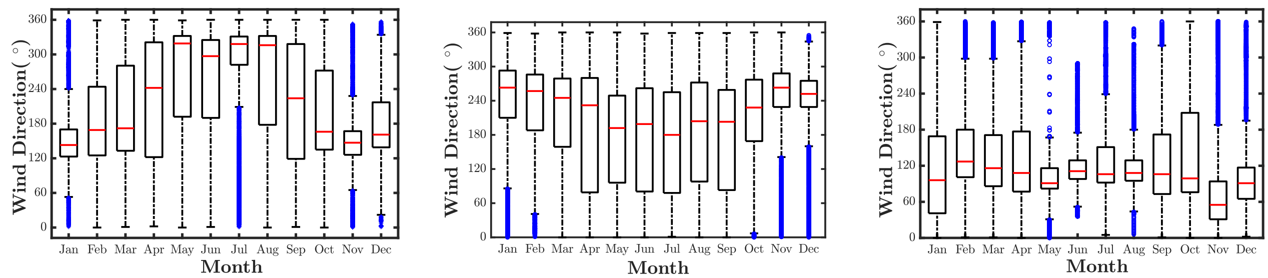

(a) Medford (Oregon) (b) Denver (Colorado) (c) Key West (Florida)

Figure 2: Variation of wind direction in different cities.

to avoid collisions at low energy cost. The presented algorithm can be run on UAV or over mobile edge computing according to the UAV capacity and task overhead.

B. Motivation and Contributions

Based on the reported works in [6] [7] [8], and [12], it is noted that the UAV velocity (both magnitude and direction), the obstacle velocity, and the distance between the UAV and the obstacle play a key role in UAV collision avoidance. However, these works do not consider the effect of wind in their frameworks. The consideration of wind is important because the UAV has to travel several kilometres of zigzag trajectory in different directions, and the effective velocity of the UAV changes in the presence of wind during the trajectory. To illustrate the effect of wind, the variation of wind profile, i.e., speed and direction, for three different cities of the USA (Medford, Denver, and Key West) is shown in Fig. 1 and Fig. 2, respectively [19]. One can observe that the profile of wind varies with space and time, and the wind speed is significant compared to the typical speed of the UAV movement, so it cannot be ignored. Not accounting for the effect of wind in the UAV collision avoidance mechanism will lead to either an accident (when the effective speed of the UAV is higher than the actual speed of the UAV) or a delay in the service (when the effective speed of the UAV is less than the actual speed of UAV). Therefore, considering the effect of wind is critical for an accurate collision avoidance system design.

The key contributions of this work are as follows: (i) A framework is presented to model the two important collision avoidance parameters, namely semiapex angle and turning radius, by considering the effect of wind speed and direction. (ii) The wind is random in nature, and hence a simple discrete-time Markov chain is used to model the semiapex angle and turning radius in a stochastic sense, using which the probability of collision avoidance is estimated. (iii) For illustrative numerical performance evaluation, we have considered the real-life wind data for three different cities of the USA (Medford, Denver, and Key West) situated at diverse geographical locations. For the UAV speed of 10m/s, the collision avoidance probability in the presence of wind is $1, 0.93$, and 0.78 for Medford, Denver, and Key West, respectively.

II. Modeling of Wind Behaviour and Its Effect on UAV Collision Avoidance

Considering aerodynamic constraints is of utmost importance in UAV path planning to ensure a collision-free flight path. For an object in motion, such as a UAV, a sufficient distance is required to make a safe turn, called the *minimum turning radius* [8]. Furthermore, the turning angle should be such that the moving object can steer away from the obstacle safely, and this angle is called *semiapex angle*. Thus, a UAV has to turn from a sufficient distance at an appropriate angle to avoid collision if it detects an obstacle. In a practical deployment scenario, the wind flow changes the velocity of the UAV, which cannot be ignored due to the ubiquitous presence of wind. This leads to a change in the above-mentioned collision avoidance parameters, which must be modeled to avoid collision. In this work, these two parameters are estimated in the presence of wind for a static obstacle. The consideration of moving obstacles lies in the scope of our future work.

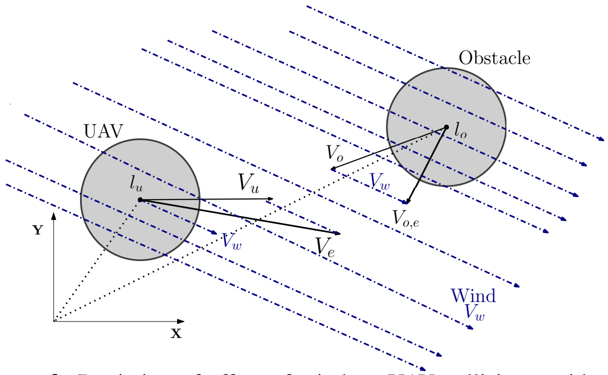

Figure 3: Depiction of effect of wind on UAV collision avoidance.

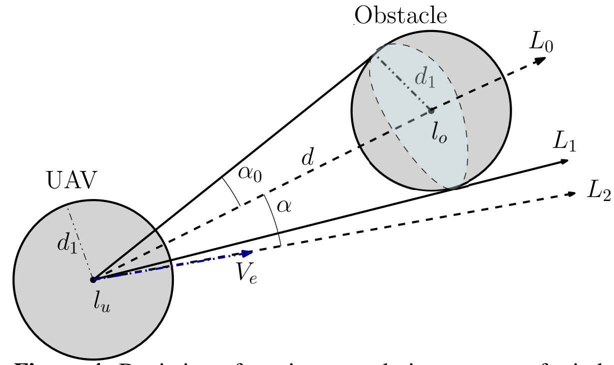

Figure 4: Depiction of semiapex angle in presence of wind.

A. *Effect of Wind*

The wind components expressed in terms of orthogonal velocity components, where W_x is along the X axis and W_y is along the Y axis, are calculated as

$$W_x = V_w \cos(\phi_m), \;\; W_y = V_w \sin(\phi_m). \tag{1}$$

where V_w is the wind velocity and ϕ_m is its direction.

Consider that the UAV is moving with speed V_u in the direction ω at a given altitude, as shown in Fig. 3. Then, its velocity component along X axis (V_u^x) and Y axis (V_u^y) in the Cartesian coordinate system are

$$V_u^x = V_u \cos(\omega), \;\; V_u^y = V_u \sin(\omega). \tag{2}$$

The velocity of UAV is affected by the presence of wind and the effective velocity of UAV, V_e, is given as [20]

$$V_e^x = V_u^x + W_x, \;\; V_e^y = V_u^y + W_y. \tag{3}$$

where V_e^x and V_e^y denote the X and Y components of V_e.

The effective velocity of the UAV can be rewritten as

$$\begin{bmatrix} V_e^x \\ V_e^y \end{bmatrix} = \begin{bmatrix} V_u^x \\ V_u^y \end{bmatrix} + \begin{bmatrix} W_x \\ W_y \end{bmatrix}. \tag{4}$$

Here, the UAV is moving at a fixed altitude, and the z-component of velocity is not taken into consideration. Three-dimensional UAV maneuverability for collision avoidance is a practical extension, which will be taken up as an extension exercise.

B. *Semiapex Angle*

Let the straight-line distance between the UAV and the obstacle be d (Fig. 4). The UAV, as well as the obstacle, is assumed to have spherical shape of radius d_1. Let l_o and l_u be the locations of the obstacle and the UAV, respectively. Then, the semiapex angle α_0, which is the angle between vectors L_0 and L_1, is given as

$$\alpha_0 = \sin^{-1}\left(\frac{d_1}{d}\right). \tag{5}$$

Now, the change in the velocity of UAV due to wind leads to a change in semiapex angle, as shown in Fig. 4. It is now the angle between the vectors L_0 and L_2 rather than the angle between L_0 and L_1. Let α denote the angle between the vectors L_0 and L_2, which is obtained as

$$\alpha = \cos^{-1}\left[\frac{\left\langle \vec{V}_r, \overrightarrow{l_{\mathrm{u}} l_o} \right\rangle}{\left|\vec{V}_r\right| \left|\overrightarrow{l_{\mathrm{UAV}} l_O}\right|}\right] \tag{6}$$

where $< \cdot >$ denotes the dot product and $\overrightarrow{l_{\mathrm{u}} l_o} = [x_o - x_u, y_o - y_u, z_o - z_u]$ is the relative location between the UAV and the obstacle with $l_o = (x_o, y_o, z_o)$ and $l_u = (x_u, y_u, z_u)$.

From Fig. 4, there can be two possible cases: (i) $\alpha > \alpha_0$: the UAV makes a turn with an angle such that it can avoid the collision, and (ii) $\alpha \leq \alpha_0$: the turn made by the UAV leads to a collision with the obstacle. Here, α_0 is a deterministic quantity, which depends upon the obstacle sphere and the distance between the UAV and the obstacle. In contrast, α depends upon the UAV and the obstacle positions, the wind profile, and UAV velocity.

C. *Turning Radius*

The minimum turning radius (R) is given as [8]

$$R = \frac{{V_e}^2}{g \tan \varphi_{\max}}. \tag{7}$$

where g and ϕ_{max} are the gravitational coefficient and the maximum roll angle.

III. Estimation of Collision Avoidance Probability

In order to investigate the effect of wind on UAV collision, the wind data of four years (2018-2022) with a temporal resolution of five minutes from three cities in the USA (Medford (Oregon), Denver (Colorado), and Key West (Florida)) available at National Renewable Energy Laboratory (NREL) [19] is used. These three cities represent varying wind conditions over different geographical locations, as shown in Fig. 1 and Fig. 2. In the dataset, the wind data comprises horizontal wind speed (V_w) and meteorological wind direction (ϕ_{met}). The meteorological wind direction is converted into the mathematical convention (ϕ_m) in order to analyze the system in Cartesian co-ordinate system as [21]:

$$\phi_m = |270 - \phi_{met}|_{360}. \tag{8}$$

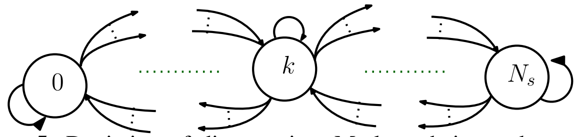

Figure 5: Depiction of discrete-time Markov chain used to model semiapex angle.

where $|\cdot|_{360}$ denotes the modulo 360 operation.

The work in [22] assumes the wind speed at a given height to be an ergodic random process, combining constant wind speed (the mean value of all data samples) and the turbulence component. Then, the turbulence component is modeled as a random variable. However, capturing the variation of wind data through some distribution is difficult as it strongly depends upon the geographic locations and rapidly changing weather conditions. Further, the wind has magnitude as well as direction in the given context, and modeling only the wind speed is not enough. Here in the given context, semiapex angle (see (6)) and turning radius (see (7)) both depend upon the effective velocity of the UAV (see (4)), which is a combination of wind velocity and UAV velocity. Therefore, a discrete-time Markov process based model is presented here; it is widely used in the literature to model the random process [23].

A. Discrete-Time Markov Chain Model

The effective velocity for each dataset sample is estimated from (4) using the given UAV velocity. Then, using (6) and (4), a sequence of values of α is obtained for each sample of the dataset. Let the value of α lie in the range $\alpha \in [\alpha_{min}, \alpha_{max}]$ with a step size Δ. Then, the number of states N_s in the Markov chain is given as

$$N_s = \lceil \frac{\alpha_{max}}{\Delta} \rceil - \lfloor \frac{\alpha_{min}}{\Delta} \rfloor + 1. \tag{9}$$

Here $\frac{\alpha_{min}}{\Delta}$ and $\frac{\alpha_{max}}{\Delta}$ denote the quantized semiapex level of the first and last state, respectively. As shown in Fig. 5, a Markov chain is formed. The transition probability matrix is now estimated to quantify the likelihood of transitioning from one state to another. Then, the steady-state probabilities of this Markov chain are estimated. The variation of cumulative distribution function (CDF) of the semiapex angle is shown in Fig. 6. It may be noted that the semiapex angle varies significantly in the range of $[0°, 42°]$, which justifies the inclusion of wind data in system design.

Likewise, the modeling of turning radius is performed. The sequence of turning radius is estimated from (7). Then, the Markov chain is formed for the obtained sequence of values of R. Using the wind data and the analysis done in Section II, the CDF of R is estimated, which is shown in Fig. 7. The turning radius shows significant variation within the range of 10 m to 67 m. Notably, when the effect of wind is ignored, the turning radius is approximately 27 m. Thus, an ideal system design does not guarantee collision avoidance and justifies the need to consider the wind in the UAV collision avoidance system design.

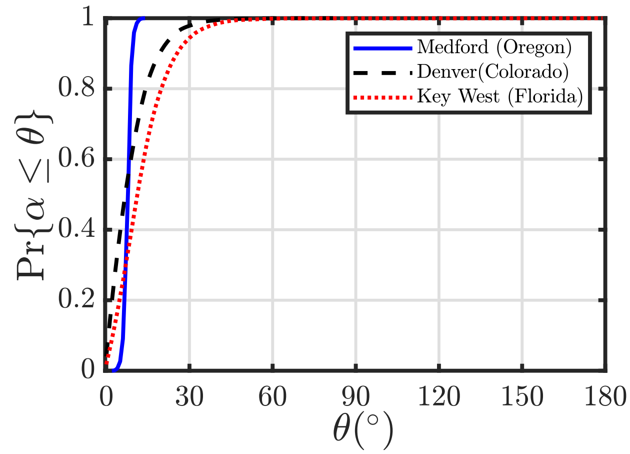

Figure 6: Variation of CDF of semiapex angle α.

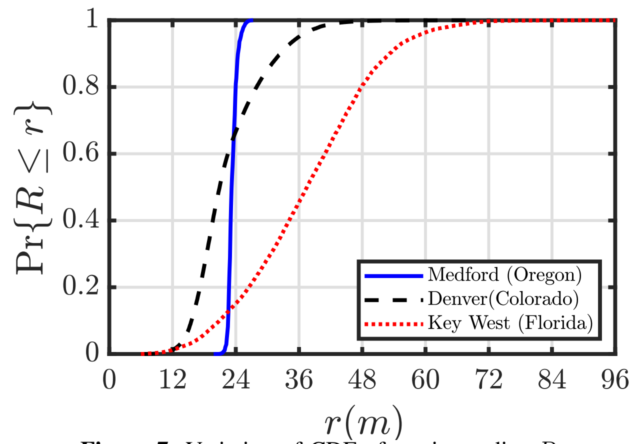

Figure 7: Variation of CDF of turning radius R.

B. Estimation of Collision Avoidance Probability

Till now, the semiapex angle and the turning radius parameters are characterized, and their distributions are estimated. The critical parameter of interest is the probability of collision avoidance (P_{CA}). Based on the basic definition of the turning radius and the system model in Fig. 4, there are two cases as depicted in Fig. 8. (i) $R \geq d$: here the UAV does not have the sufficient spatial margin to take the turn safely; therefore, UAV

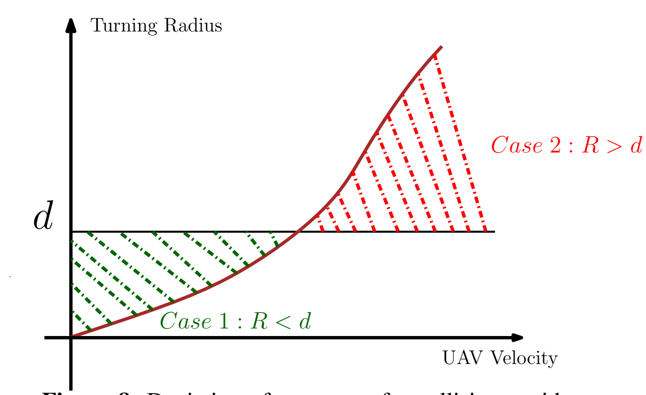

Figure 8: Depiction of two cases for collision avoidance.

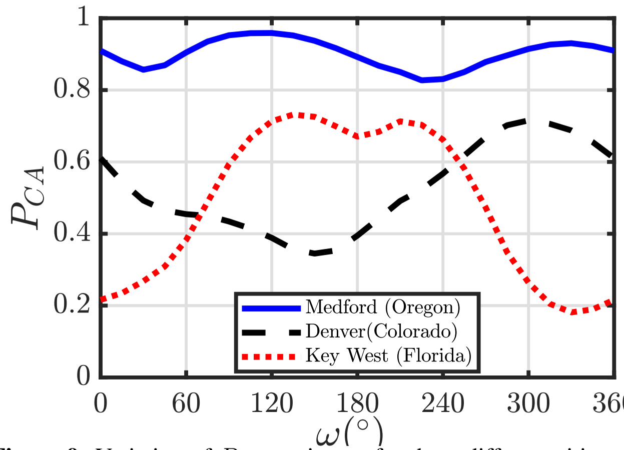

Figure 9: Variation of P_{CA} against ω for three different cities with $d = 40$ m, $d_1 = 1$ m, and $V_u = 10$ m/s.

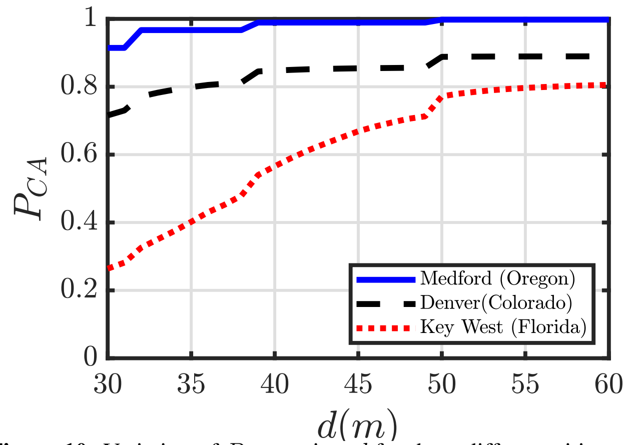

Figure 10: Variation of P_{CA} against d for three different cities with $\omega = 30^\circ$, $d_1 = 1$ m, and $V_u = 10$ m/s.

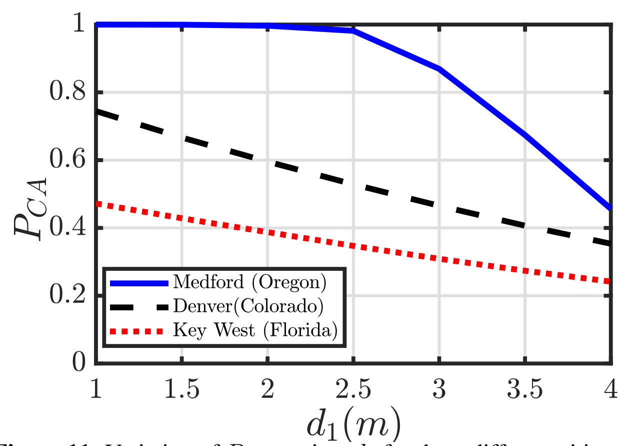

Figure 11: Variation of P_{CA} against d_1 for three different cities with $\omega = 30^\circ$, $d = 40$ m, and $V_u = 10$ m/s.

collides with the obstacle, and (ii) $R < d$: here the collision will not take place as the UAV has a sufficient spatial margin for safe turn. Similarly, from the basic definition of semiapex angle and the system model shown in Fig. 4, two cases exist. (i) $\alpha \leq \alpha_0$: here the semiapex angle is not enough; the UAV will collide with the obstacle, and (ii) $\alpha > \alpha_0$: here the UAV has sufficient angular margin, so it can pass the object safely.

Based on the above discussion, the collision can only be avoided when the UAV has sufficient spatial distance to make a safe turn, i.e., $R < d$, and enough angular margin, i.e., $\alpha > \alpha_0$. Thus, P_{CA} is computed as

$$P_{CA} = \Pr\{R < d\} \cdot \Pr\{\alpha > \alpha_0\}. \tag{10}$$

where Pr denotes the probability.

P_{CA} can be rewritten as

$$P_{CA} = F_R(d) \cdot (1 - F_\alpha(\alpha_0)). \tag{11}$$

where $F_R(\cdot)$ and $F_\alpha(\cdot)$ respectively denote the CDF of turning radius and semiapex angle, which are obtained using the discrete-time Markov chain model discussed in Section III-A.

IV. Results and Discussion

We have done the performance analysis for 15 cities in the USA to investigate the impact of wind. We observed that the value of P_{CA} significantly decreases for all these cities. However, for numerical illustration, we present the performance evaluation of three USA cities (Medford, Denver, and Key West) situated at different geographical locations. The wind data has a resolution of five minutes. The simulation considers $g = 9.8$ m/s^2, $\varphi_{\max} = 30^\circ$, and step sizes ($\Delta$) of 1° for the semiapex angle and 0.5 m for the turning radius.

Variation of collision avoidance probability, P_{CA}, against the angle of movement of UAV, ω, is shown in Fig. 9 for three cities. One can observe that P_{CA} varies significantly with ω for all three cities. This happens because whenever the wind direction is aligned with ω, the effective velocity of the UAV increases, and P_{CA} decreases. This plot also indicates that the value of P_{CA} in the presence of wind is much lesser than ideal case 1, i.e., in the absence of wind [6]–[8], [12]. The P_{CA} variation against the straight-line distance between the UAV and the obstacle, d, is shown in Fig. 10. It may be noted that P_{CA} increases significantly with an increase in d because the UAV gets sufficient distance to make a safe turn. Further, the semiapex angle α_0 is relatively small for higher d, further reducing the chances of collision.

Remark 1. *In the UAV collision avoidance mechanism, not accounting for the effect of wind will lead to inaccurate system design, which may have severe consequences.*

The effect of the dimension of the obstacle, d_1 is depicted in Fig. 11. It may be noted that P_{CA} value decreases as the dimension of the obstacle increases because α_0 increases with an increase in d_1. This leads to the reduced value of $\Pr\{\alpha > \alpha_0\}$, and chances of collision increase. The effect of the speed of the UAV is depicted in Fig. 12, which shows the variation of P_{CA} against the UAV velocity V_u. Here, P_{CA} value is found to decrease with an increase in the UAV speed because higher speed leads to a relatively larger turning radius, which decreases the chances of collision (see case 1 of Fig. 8). From

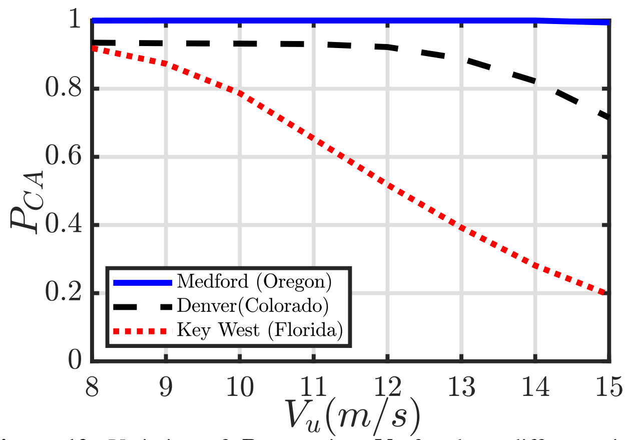

Figure 12: Variation of P_{CA} against V_u for three different cities with $\omega = 30^{\circ}$, $d = 40$ m, and $d_1 = 1$ m/s.

Fig. 12, it may also be noted that P_{CA} value is not found to decrease with V_u for Medford because the wind speed is negligible for Medford (see Fig. 1).

Remark 2. *The UAV must be aware of its direction and speed of movement, the wind profile, the dimension of the obstacle, and the distance from the obstacle while making the turn to avoid collision.*

V. Conclusions

This work presents a framework to capture the effect of wind on UAV collision avoidance. To this end, the effect of wind has been modeled, and it has been noted that the effective velocity of UAVs changes when the presence of random wind is taken into account. Using this model, the parameters to ensure collision avoidance, i.e., turning radius and semiapex angle, have been analyzed in the presence of wind using a discrete-time Markov chain due to the random nature of wind. Collision avoidance probability has been computed. Data from three places in the USA have been considered for numerical evaluation of the proposed framework.

Further investigations into the design of collision avoidance mechanisms in the presence of wind for different allowed hovering altitudes of interest and the use of learning-aided adaptive collision avoidance are of interest. UAV mobility trajectory design to overcome the effect of wind is another interesting direction of extension.

Acknowledgment

This work was supported in parts by the Indian National Academy of Engineering (INAE) through the Abdul Kalam Technology Innovation National Fellowship, and Start-up Research Grant (SRG), Science & Engineering Research Board (SERB), Department of Science and Technology under grant SRG/2023/002269

References

[1] M. Mozaffari, W. Saad, M. Bennis, Y.-H. Nam, and M. Debbah, "A tutorial on UAVs for wireless networks: Applications, challenges, and open problems," *IEEE Commun. Surveys Tuts.*, vol. 21, no. 3, pp. 2334–2360, thirdquarter, 2019.

[2] GVR, "Commercial drone market size, share & trends analysis report, 2023 - 2030," Grand View Research, Inc. San Francisco, CA, United States, Tech. Rep., 2023.

[3] Unmanned aircraft systems (UAS), federal aviation administration (FAA), Washington, D.C., USA. [Online]. Available: www.faa.gov/uas

[4] The Drone Rules 2021, Directorate General of Civil Aviation (DGCA), New Delhi, India.

[5] E. Vinogradov, F. Minucci, and S. Pollin, "Wireless communication for safe UAVs: From long-range deconfliction to short-range collision avoidance," *IEEE Veh. Technol.*, vol. 15, no. 2, pp. 88–95, June 2020.

[6] Y. Fu, X. Yu, and Y. Zhang, "Sense and collision avoidance of unmanned aerial vehicles using markov decision process and flatness approach," in *Proc. IEEE Int. Conf. Inf. Autom.*, 2015, pp. 714–719.

[7] P. P.-Y. Wu, D. Campbell, and T. Merz, "Multi-objective four-dimensional vehicle motion planning in large dynamic environments," *IEEE Trans. Syst., Man, Cybern. B, Cybern.*, vol. 41, no. 3, pp. 621–634, June, 2011.

[8] X. Zhou, X. Yu, and X. Peng, "UAV collision avoidance based on varying cells strategy," *IEEE Aerosp. Electron. Syst.*, vol. 55, no. 4, pp. 1743–1755, Aug., 2019.

[9] J.-H. Chuang and N. Ahuja, "An analytically tractable potential field model of free space and its application in obstacle avoidance," *IEEE Trans. Syst., Man, Cybern. B, Cybern.*, vol. 28, no. 5, pp. 729–736, Oct., 1998.

[10] Y. Fu, Y. Zhang, and X. Yu, "An advanced sense and collision avoidance strategy for unmanned aerial vehicles in landing phase," *IEEE Aerosp. Electron. Syst. Mag.*, vol. 31, no. 9, pp. 40–52, Sept., 2016.

[11] F. Minucci, E. Vinogradov, and S. Pollin, "Avoiding collisions at any (low) cost: ADS-B like position broadcast for UAVs," *IEEE Access*, vol. 8, pp. 121 843–121 857, July, 2020.

[12] J. Seo, Y. Kim, S. Kim, and A. Tsourdos, "Collision avoidance strategies for unmanned aerial vehicles in formation flight," *IEEE Aerosp. Electron. Syst.*, vol. 53, no. 6, pp. 2718–2734, Dec., 2017.

[13] Q. Quan, R. Fu, and K.-Y. Cai, "How far two UAVs should be subject to communication uncertainties," *IEEE Trans. Intell. Transp. Syst.*, vol. 24, no. 1, pp. 429–445, Jan., 2023.

[14] J. Park and Y. Kim, "Collision avoidance for quadrotor using stereo vision depth maps," *IEEE Aerosp. Electron. Syst.*, vol. 51, no. 4, pp. 3226–3241, Oct., 2015.

[15] A. K. Mandal, J.-B. Seo, S. De, A. K. Poddar, and U. Rohde, "A novel statistically-aided learning framework for precise localization of uavs," in *IEEE Veh. Tech. Conf. (VTC2023-Spring)*, 2023, pp. 1–5.

[16] D. Wang, T. Fan, T. Han, and J. Pan, "A two-stage reinforcement learning approach for multi-UAV collision avoidance under imperfect sensing," *IEEE Robot. Autom. Lett.*, vol. 5, no. 2, pp. 3098–3105, April, 2020.

[17] A. Singla, S. Padakandla, and S. Bhatnagar, "Memory-based deep reinforcement learning for obstacle avoidance in UAV with limited environment knowledge," *IEEE Trans. Intell. Transp. Syst.*, vol. 22, no. 1, pp. 107–118, Jan., 2021.

[18] S. Ouahouah, M. Bagaa, J. Prados-Garzon, and T. Taleb, "Deep-reinforcement-learning-based collision avoidance in UAV environment," *IEEE Internet Things J.*, vol. 9, no. 6, pp. 4015–4030, Oct., 2022.

[19] C. Draxl, A. Clifton, B.-M. Hodge, and J. McCaa, "The wind integration national dataset (wind) toolkit," *Applied Energy*, vol. 151, pp. 355–366, 2015.

[20] T. Souanef, "$\mathcal{L}_1$ adaptive path-following of small fixed-wing unmanned aerial vehicles in wind," *IEEE Aerosp. Electron. Syst.*, vol. 58, no. 4, pp. 3708–3716, 2022.

[21] J. M. Wallace and P. V. Hobbs, *Atmospheric science: an introductory survey*. Elsevier, 2006, vol. 92.

[22] J. Chen, M. C. Hui, and Y. L. Xu, "A comparative study of stationary and non-stationary wind models using field measurements," *Boundary-layer meteorology*, vol. 122, pp. 105–121, 2007.

[23] S. Suman and S. De, "Solar-enabled green base stations: Cost versus utility," in *IEEE Int. Symp. World Wireless Mobile Multimedia Netw. (WoWMoM)*, June, 2017, pp. 1–8.